FDTD-based CAD Simulator for Coaxial Applicator — Biomedical Application

C. W. Lee[1], **K. Y. You**[1], **and C. Y. Lee**[2]

[1]Department Communication Engineering, Faculty of Electrical Engineering
Universiti Teknologi Malaysia, Skudai 81310, Malaysia
[2]Faculty of Bioscience and Medical Engineering
Universiti Teknologi Malaysia (UTM), Johor 81310, Malaysia

Abstract— This paper presents development of FDTD-based CAD simulator using MATLAB graphic user interface feature for solving the coaxial applicator problem. The capability of the CAD is to visualize the 2D and 3D electromagnetic field and bio-heat distribution. The CAD is competitive with commercial simulator in term of learning curve and simplicity in the program algorithm. In this paper, the creation steps of the CAD are described in detail. In addition, the comparison result between the CAD and commercial simulator are intensively discussed and analyzed. Some of the improvements of this CAD are also presented.

1. INTRODUCTION

Simulator is gaining importance nowadays for scientists and researchers to complete their research work. However, commercial simulator is costly. There exist few free open-source simulators [1] and those are not user friendly. Here, we attempt to develop simple graphical user interface (GUI) to overcome the above issue. In this paper, we only focused on Finite Difference Method (FDM) [2] and Finite Difference Time-Domain (FDTD) [3] which was applied to the coaxial type applicator in hyperthermia treatment. Coaxial applicator becomes popular due to its thin slot form and small cross section area which can realize minimal invasive treatment such as deep seated brain tumor.

2. THEORECTICAL BACKGROUND

All the solutions to the problem of electromagnetic are always refer to the Maxwell's equation. Here, the FDTD is applied on coated monopole applicator to solve an electromagnetic (EM) fields using the Maxwell's equations in time, t domain and cylindrical coordinate (ρ, $\varnothing$ and z) [4]:

$$\frac{\partial E_\rho}{\partial z} - \frac{\partial E_z}{\partial \rho} = -\mu_o \frac{\partial H_\phi}{\partial t} + \sigma H_\phi \tag{1a}$$

$$-\frac{\partial H_\phi}{\partial z} = -\varepsilon_o \varepsilon_r \frac{\partial E_\rho}{\partial t} + \sigma E_\rho \tag{1b}$$

$$\frac{1}{\rho}\frac{\partial(\rho H_\phi)}{\partial \rho} = -\varepsilon_o \varepsilon_r \frac{\partial E_z}{\partial t} + \sigma E_z \tag{1c}$$

where E_ρ, E_z and $H_\varnothing$ are the radial, axial electric fields (V/m) and azimuth magnetic field (A/m), respectively. Symbols μ_o and ε_o are the permeability (H/m) and permittivity (F/m) of free space, while, ε_r and σ are the relative permittivity and conductivity (S/m) of ambient medium. While, the scatter heat distribution due to EM energy along the length of coated monopole driven from coaxial line, was solved by FDM. The governing Pennes' bioheat transfer equation [5] was used and given as:

$$pC_p \frac{\partial T}{\partial t} = K\left(\frac{\partial^2 T}{\partial \rho^2} + \frac{1}{\rho}\frac{\partial T}{\partial \rho} + \frac{\partial^2 T}{\partial z^2}\right) - \omega_b C_b p_b (T - T_a) + Q_{met} + Q_{ext} \tag{2}$$

where T is the final temperature (°C) in biological medium; T_a is the arterial temperature (°C). Symbols p, C_p and K are the density (kg/m^3), specific heat capacity (J/(kg°C)) and thermal conductivity (W/(m°C)) of the biological medium, respectively; Symbols p_b and C_b are the density (kg/m^3) and specific heat capacity (J/(kg°C) of blood, respectively; ω_b is the blood perfusion rate (m^3/(kg · s)), which is assumed to be constant; Q_{met} is the metabolic heat generation rate (ignored in this study) and Q_{ext} is the external heat sources which is related to electric field, E, as:

$$SAR = \frac{\sigma |E|^2}{2p} = \frac{Q_{ext}}{p} \tag{3}$$

where SAR is the specific absorption rate (W/kg) of biological medium. In FDTD routine, the (1) is required to convert into discrete form as:

$$H_\phi^{n+0.5}(i,j) = H_\phi^{n-0.5}(i,j)+\frac{\Delta t}{\mu_0}\left[\frac{E_\rho^n(i,j+0.5)-E_\rho^n(i,j-0.5)}{\Delta z}\right] - \frac{\Delta t}{\mu_0}\left[\frac{E_z^n(i+0.5,j)-E_z^n(i-0.5,j)}{\Delta\rho}\right] \quad (4a)$$

$$E_z^{n+1}(i+0.5,j) = \frac{\left(1-\frac{\sigma\Delta t}{2\varepsilon_o\varepsilon_r}\right)}{\left(1+\frac{\sigma\Delta t}{2\varepsilon_o\varepsilon_r}\right)}E_z^n(i+0.5,j)+\frac{\frac{\Delta t}{\varepsilon_o\varepsilon_r}}{\left(1+\frac{\sigma\Delta t}{2\varepsilon_o\varepsilon_r}\right)}\left[\frac{\rho_{i+1}H_\phi^{n+0.5}(i+1,j)-\rho_i H_\phi^{n+0.5}(i,j)}{\rho_{i+0.5}\Delta\rho}\right] \quad (4b)$$

$$E_\rho^{n+1}(i,j-0.5) = \frac{\left(1-\frac{\sigma\Delta t}{2\varepsilon_o\varepsilon_r}\right)}{\left(1+\frac{\sigma\Delta t}{2\varepsilon_o\varepsilon_r}\right)}E_\rho^n(i,j-0.5)-\frac{\frac{\Delta t}{\varepsilon_0\varepsilon_r}}{\left(1+\frac{\sigma\Delta t}{2\varepsilon_o\varepsilon_r}\right)}\left[\frac{H_\phi^{n+0.5}(i,j)-H_\phi^{n+0.5}(i,j-1)}{\Delta z}\right] \quad (4c)$$

Similarly, for FDM, the (2) is discretized as:

$$\frac{\partial T}{\partial t} = \frac{K}{pc}\left[\frac{T(i+1,j)-2T(i,j)+T(i-1,j)}{\Delta\rho^2}+\frac{1}{\rho}\frac{T(i+1,j)-T(i,j)}{2\Delta\rho}+\frac{T(i+1,j)-2T(i,j)+T(i-1,j)}{\Delta z^2}\right] - \frac{\omega_b c_b p_b}{pc}\left[T(i,j)-T_a\right]+\frac{SAR}{c} \quad (5)$$

The Equation (5) is further solved explicitly by available MATLAB ode45 solver [6].

3. RESULTS AND ANALYSIS

3.1. Simulated Configuration

This study simulator considers the coated monopole driven from coaxial line as axis symmetrical in order to reduce the computational resource and run time. Source is fed from the end of the coaxial line and it is assume to be TEM along the coaxial line. Soft source is used to allow reflected wave to be absorbed. Since FDTD operates in time domain, differentiated Gaussian pulse excitation is performed. When steady-state is reached, Fourier transform is used to obtain frequency response. The domain for the analysis is truncated with perfectly matched layer (PML) based on recursive convolution and the use of complex frequency shifted (CFS) parameters to absorb all outgoing electromagnetic waves. To ensure stability, time step set adhere to "Courant-Friedrichs-Lewy condition", which is described in detail in [4]. Grid cell, $\Delta\rho$ used is 0.25 mm equivalent to 75 points per wavelength to reduce numerical dispersion error. The type of applicator to be used in this study is a thin monopole used in hyperthermia treatment coated with catheter made of Teflon. There exist thin air gap between the catheter and the conductor as shown in Figure 1. The height of the monopole is set to $\beta_L h = \pi/4$ at $f = 915$ MHz. The values of initial parameters of the study simulation are given in Table 1. Up to 10 watt power is introduced through the coaxial line for three minutes to obtain the final temperature.

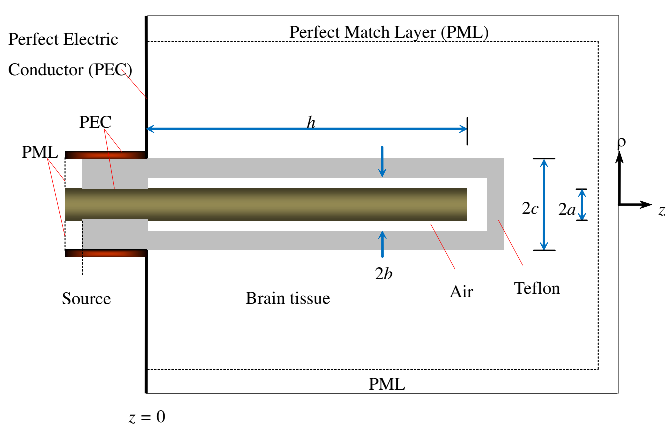

Figure 1: Geometry of coated monopole.

Table 1: Parameters in the FDTD simulation.

Dimensions of monopole	Dielectric Properties of Mediums	Thermal Properties of Mediums	
$a = 0.5\,\mathrm{mm}$	Air: $\varepsilon_r = 1$	Brain Tissue: $K = 0.497\,\mathrm{W/(m^\circ C)}$	Blood: $K = 0.45\,\mathrm{W/(m^\circ C)}$
$b = 0.75\,\mathrm{mm}$	Teflon: $\varepsilon_r = 2.06$	$p = 1030\,\mathrm{kg/m^3}$	$p = 1058\,\mathrm{kg/m^3}$
$c = 1.5\,\mathrm{mm}$	Brain Tissue: $\varepsilon_r = 42.5$	$C_p = 3600\,\mathrm{J/(kg^\circ C)}$	$C_p = 3960\,\mathrm{J/(kg^\circ C)}$
$h = 21.1\,\mathrm{mm}$	$\sigma = 0.88\,\mathrm{S/m}$		

3.2. GUI Features

GUI developed is simple and straight forward where it is made up of a graphic display, 6 function buttons and a display drop down list as shown in Figure 2. Comparison with COMSOL's GUI is shown in Figure 3.

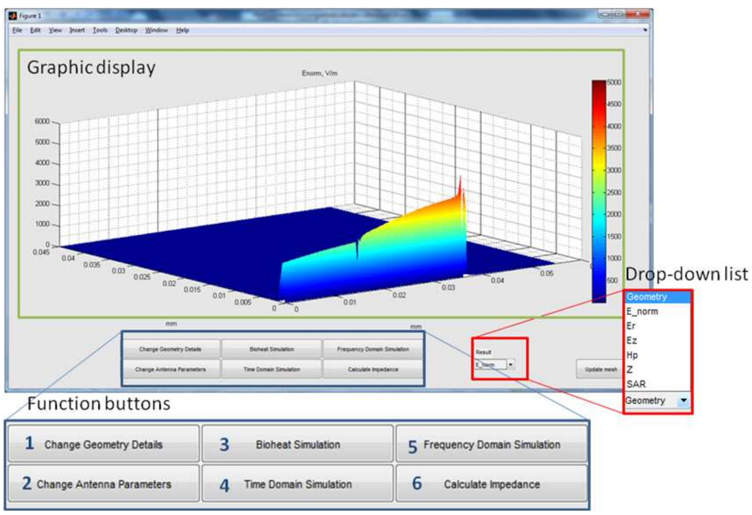

Figure 2: Developed simulator's GUI components.

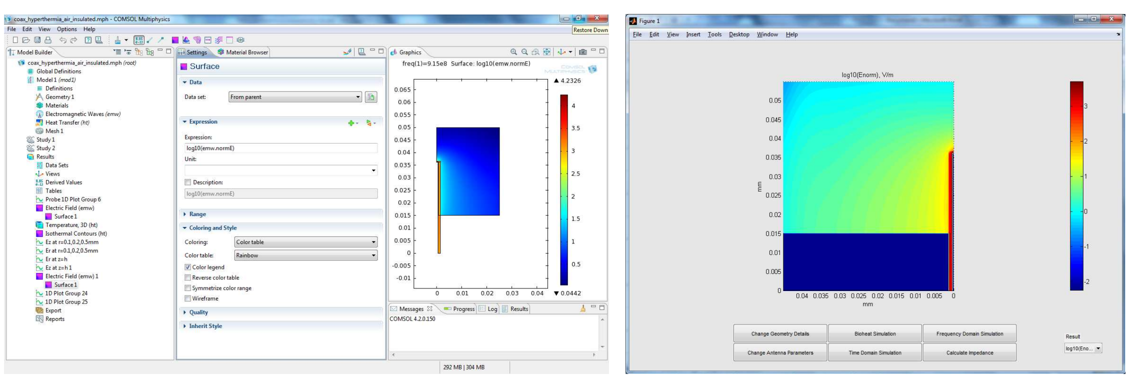

(a) (b)

Figure 3: (a) COMSOL's GUI. (b) Developed simulator's GUI.

3.2.1. Graphic Display

Results and geometry model are plotted at a time on the graphic display base on the option selected in the drop-down list.

3.2.2. Drop-down List

There are 7 types of result to be selected from the drop down list which are geometry model, normalized electric field, axial and radial electric field, azimuth magnetic field, input impedance, and SAR distribution.

3.2.3. Function Buttons

When function buttons are pressed, a dialog box is launched for assignment of respective parameters. To save the changes, press the OK button and respective simulation is performed.

1. "**Change Geometry Detail**" button is used to define the grid cell size, simulation domain size, number of PML layers, and biological medium properties.
2. "**Change Antenna Parameters**" button is used to define the antenna dimensions and material properties.
3. "**Bioheat Simulation**" button is used to solve bioheat equation and the final solution is interpreted in temperature distribution. Duration of the simulation and thermal properties of the biological and blood medium is defined in the dialog box.
4. "**Time Domain Simulation**" button will initiate real time animation of the electric field wave propagation. Type of source, frequency of interest, input voltage and maximum number of time steps can be defined in the dialog box.
5. "**Frequency Domain Simulation**" button is capable of calculating the electric and magnetic field distribution in frequency domain. Dialog box shown similar parameters as from button 4.
6. "**Calculate Impedance**" button is used to calculate variation of impedance with frequency. Parameters to be defined are range of frequencies, maximum number of time steps and type of source.

3.3. Results Discussion

In this section, the computed electric field, (E_ρ and E_z) and input impedance, Z_{in} at driving point are validated against analytical solution [7] and COMSOL simulation results. Electric field is compared at 6 different cross sections parallel to ρ-axis and z-axis. Due to differences excitation sources were respectively used by the three approaches, thus, the computed results are normalized to its maximum value for ease of comparison. The results of the radial and axial components of the electric field are plotted in Figure 4 and Figure 5, respectively.

Near the boundary of the domain, less efficient PML used will cause significantly small reflection back to the domain which can be seen in Figure 4(a). Analytical method is not susceptible to this problem, thus small difference is noticeable between analytical solution with COMSOL and FDTD near the end of $\rho = 10$ mm and. COMSOL method which shows more deviation than FDTD toward analytical method has less efficient PML. Secondly, Figure 5(a) shows that large difference between FDTD with analytical method at $z = 1.1$ mm, but good agreement with COMSOL simulation. The difference is due to the absence of fringing effect in analytical solution. Also in Figure 5(b), considerable difference with FEM and analytical is noticeable at $z = 21.1$ mm, mainly due to strong forces at the tip. Overall the agreement between simulator's results with 2 other methods is good.

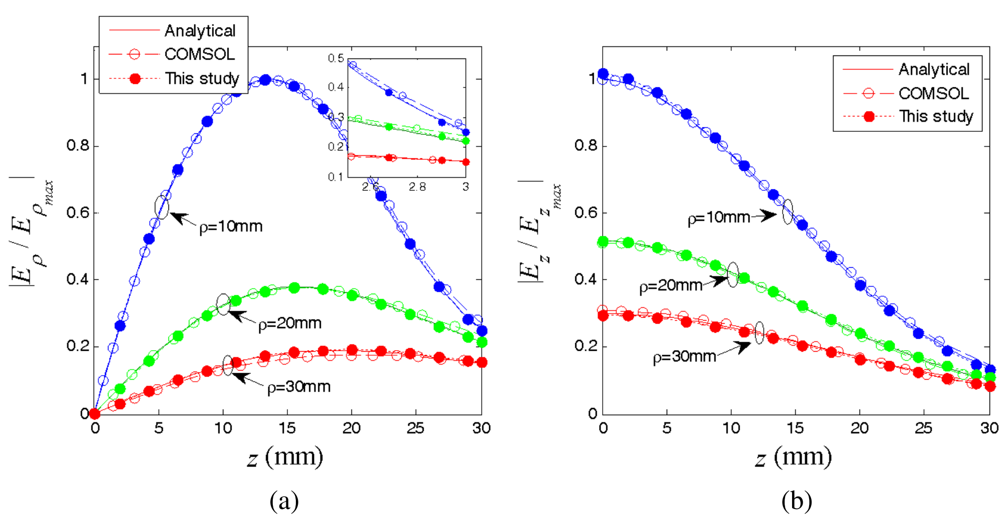

Figure 4: Electric field near insulated monopole normalized to maximum at cross section parallel to z-axis. (a) E_ρ and (b) E_z.

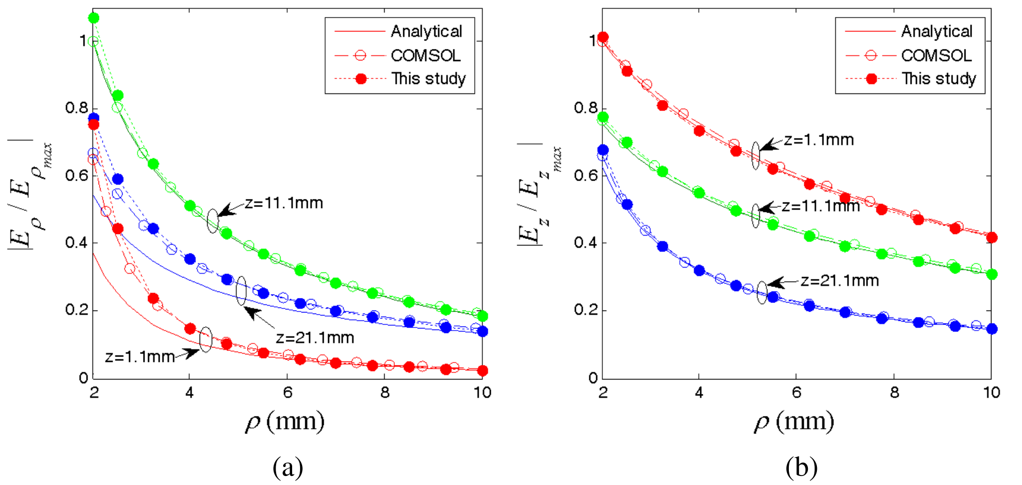

Figure 5: Electric field near insulated monopole normalized to maximum at cross section parallel to ρ-axis. (a) E_ρ and (b) E_z.

Input impedance, Z_{in} at driving point ($z = 0$) for analytical solution is obtained from characteristic impedance using the simple transmission line theory [7] and further corrected for its fringing effect. Comparison is made from 1 GHz to 8 GHz and plotted in Figure 6. Simulator's result agrees very well with FEM solution but deviate slightly in reactance, X_{in} at frequency higher than 5 GHz with analytical solution.

Comparison of temperature contour at 43°C surrounding monopole between the FDTD computed results and the COMSOL simulated results was shown in Figure 7. 43°C is the therapeutic temperature for effective hyperthermia treatment. From Figure 7, small difference is noticeable near the tip of the antenna. This is expected as rapid field growth is expected around that region.

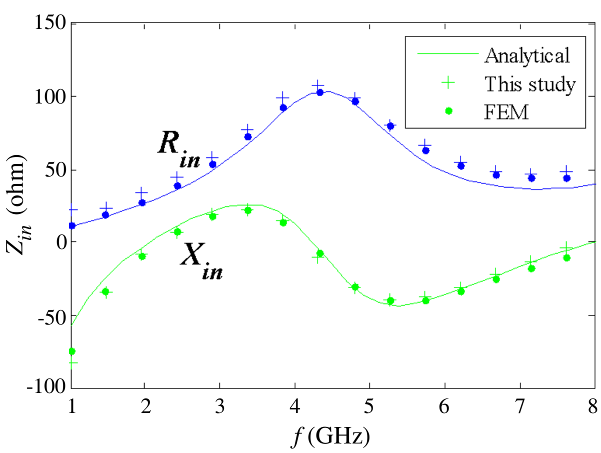

Figure 6: Comparison of simulator's result with analytical solution and FEM method.

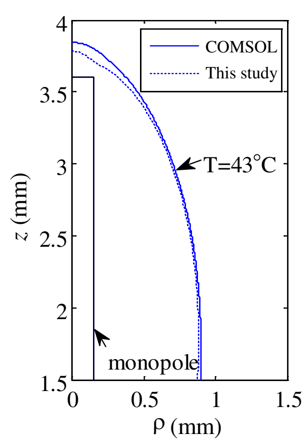

Figure 7: Comparison of temperature contour at 43°C with COMSOL simulation.

4. SIMULATOR'S LIMITATIONS

For the time being, simulator developed is not full-featured where it doesn't support anisotropic material, periodic boundary condition and other excitation mode such as transverse electric (TE) mode. Besides, only uniform grid size can be defined that further compromise the run time of simulation. For example in this study, fine mesh of 0.25 mm is used due to constraint of narrow air gap geometry between catheter and conductor. In fact, non uniform grid size will enable finer mesh defined at critical solution areas (area surrounding the tip and aperture of the monopole), while coarser mesh defined at other solution regions.

5. CONCLUSION

In this study, a FDTD-based simulator with simple GUI specifically caters for coaxial applicator was successfully developed. In future, the limitations above will be improved.

ACKNOWLEDGMENT

This study was supported by the Universiti Teknologi Malaysia and Ministry of Higher Education (MOHE) Malaysia under project number Q.J130000.2523.04H77.

REFERENCES

1. Liebig, T., et al., "OpenEMS — A free and open source equivalent-circuit (EC) FDTD simulation platform supporting cylindrical coordinates suitable for the analysis of traveling wave MRI applications," *International Journal of Numerical Modelling: Electronic Networks, Devices and Fields*, Vol. 26, 680–696, 2013.
2. He, Z. Z., X. Xue, and J. Liu, "An effective finite difference method for simulation of bioheat transfer in irregular tissues," *Journal of Heat Transfer-Transactions of the Asme*, Vol. 135, 2013.
3. Sullivan, D. M., *Electromagnetic Simulation Using the FDTD Method*, John Wiley & Sons, 2013.
4. Maloney, J. G., G. S. Smith, and W. R. Scott, "Accurate computation of the radiation from simple antennas using the finite-difference time-domain method," *IEEE Transactions Antennas and Propagation*, Vol. 38, 1059–1068, 1990.
5. Wissler, E. H., "Pennes' 1948 paper revisited," *J. Appl. Physiol.*, Vol. 85, 35–41, 1998.
6. Schiesser, W. E. and G. W. Griffiths, *A Compendium of Partial Differential Equation Models: Method of Lines Analysis with Matlab,* Cambridge University Press, 2009.
7. King, R. W., B. Trembly, and J. Strohbehn, "The electromagnetic field of an insulated antenna in a conducting or dielectric medium," *IEEE Trans. Microwave Theory Tech.*, Vol. 31, 574–583, 1983.